Thermodielectric generation of defect modes in a photonic liquid crystal

Yu-Cheng Hsiao, Hsiao-Tsung Wang, and Wei Lee*

College of Photonics, National Chiao Tung University, Guiren Dist., Tainan 71150, Taiwan
wlee@nctu.edu.tw

Abstract: Photonic defect modes induced by *in situ* formation of an ill-defined defect layer is demonstrated in a cholesteric liquid crystal (CLC). The local deformation of the one-dimensionally periodic helical structure is achieved by means of the thermodielectric effect, which alters the pitch in the middle of the cholesteric structure. The defect-mode peak in the photonic band gap appears in the transmission spectrum only when the incident circularly polarized light has the same handedness as that of the CLC structure. The wavelength of the deformation-induced defect mode can be tuned upon varying the dielectric heating power by simply applying a frequency-modulated voltage.

OCIS codes: (230.3720) Liquid-crystal devices; (230.5298) Photonic crystals.

References and links

1. E. Yablonovitch, "Inhibited spontaneous emission in solid-state physics and electronics," Phys. Rev. Lett. **58**(20), 2059–2062 (1987).
2. S. John, "Strong localization of photons in certain disordered dielectric superlattices," Phys. Rev. Lett. **58**(23), 2486–2489 (1987).
3. E. Yablonovitch, T. J. Gmitter, R. D. Meade, A. M. Rappe, K. D. Brommer, and J. D. Joannopoulos, "Donor and acceptor modes in photonic band structure," Phys. Rev. Lett. **67**(24), 3380–3383 (1991).
4. J. S. Foresi, P. R. Villeneuve, J. Ferrera, E. R. Thoen, G. Steinmeyer, S. Fan, J. D. Joannopoulos, L. C. Kimerling, H. I. Smith, and E. P. Ippen, "Photonic crystals: putting a new twist on light," Nature **390**(6656), 143–149 (1997).
5. O. Painter, R. K. Lee, A. Scherer, A. Yariv, J. D. O'Brien, P. D. Dapkus, and I. Kim, "Two-dimensional photonic band-Gap defect mode laser," Science **284**(5421), 1819–1821 (1999).
6. S. Noda, A. Chutinan, and M. Imada, "Trapping and emission of photons by a single defect in a photonic bandgap structure," Nature **407**(6804), 608–610 (2000).
7. B. Park, M. Kim, S. W. Kim, and I. T. Kim, "Circularly polarized unidirectional lasing from a cholesteric liquid crystal layer on a 1-D photonic crystal substrate," Opt. Express **17**(15), 12323–12331 (2009).
8. N. Ganesh, W. Zhang, P. C. Mathias, E. Chow, J. A. N. T. Soares, V. Malyarchuk, A. D. Smith, and B. T. Cunningham, "Enhanced fluorescence emission from quantum dots on a photonic crystal surface," Nat. Nanotechnol. **2**(8), 515–520 (2007).
9. R. Ozaki, T. Matsui, M. Ozaki, and K. Yoshino, "Electro-tunable defect mode in one-dimensional periodic structure containing nematic liquid crystal as a defect layer," Jpn. J. Appl. Phys. Part 2 **41**(12B), L1482–L1484 (2002).
10. I. P. Ilchishin, L. N. Lisetski, and T. V. Mykytiuk, "Reversible phototuning of lasing frequency in dye doped cholesteric liquid crystal and ways to improve it," Opt. Mater. Express **1**(8), 1484–1493 (2011).
11. W. Lee and S.-T. Wu, "Focus issue introduction: liquid crystal materials for photonic applications," Opt. Mater. Express **1**(8), 1585–1587 (2011).
12. P. G. de Gennes and J. Prost, *The Physics of Liquid Crystals*, 2nd ed. (Oxford University, 1993).
13. Y.-C. Hsiao, C.-Y. Wu, C.-H. Chen, V. Ya. Zyryanov, and W. Lee, "Electro-optical device based on photonic structure with a dual-frequency cholesteric liquid crystal," Opt. Lett. **36**(14), 2632–2634 (2011).
14. C. Y. Wu, Y. H. Zou, I. Timofeev, Y. T. Lin, V. Y. Zyryanov, J. S. Hsu, and W. Lee, "Tunable bi-functional photonic device based on one-dimensional photonic crystal infiltrated with a bistable liquid-crystal layer," Opt. Express **19**(8), 7349–7355 (2011).
15. Y.-C. Hsiao, Y.-H. Zou, I. V. Timofeev, V. Ya. Zyryanov, and W. Lee, "Spectral modulation of a bistable liquid-crystal photonic structure by the polarization effect," Opt. Mater. Express **3**(6), 821–828 (2013).
16. M. Xu and D.-K. Yang, "Dual frequency cholesteric light shutters," Appl. Phys. Lett. **70**(6), 720–722 (1997).
17. C.-Y. Huang, K.-Y. Fu, K.-Y. Lo, and M.-S. Tsai, "Bistable transflective cholesteric light shutters," Opt. Express **11**(6), 560–565 (2003).

#203354 - $15.00 USD Received 18 Dec 2013; revised 3 Feb 2014; accepted 3 Feb 2014; published 6 Feb 2014

18. J. Ma, L. Shi, and D.-K. Yang, "Bistable polymer stabilized cholesteric texture light shutter," Appl. Phys. Express **3**(2), 021702 (2010).
19. F.-C. Lin and W. Lee, "Color-reflective dual-frequency cholesteric liquid crystal displays and their drive schemes," Appl. Phys. Express **4**(11), 112201 (2011).
20. Y.-C. Hsiao and W. Lee, "Lower operation voltage in dual-frequency cholesteric liquid crystals based on the thermodielectric effect," Opt. Express **21**(20), 23927–23933 (2013).
21. Y.-C. Hsiao, C.-Y. Tang, and W. Lee, "Fast-switching bistable cholesteric intensity modulator," Opt. Express **19**(10), 9744–9749 (2011).
22. Y.-C. Hsiao, C.-T. Hou, V. Ya. Zyryanov, and W. Lee, "Multichannel photonic devices based on tristable polymer-stabilized cholesteric textures," Opt. Express **19**(24), 23952–23957 (2011).

1. Introduction

Photonic crystals (PCs) with periodic structures have been extensively studied over the past two decades [1,2]. In a PC, the propagation of light is inhibited under the Bragg condition, resulting in the appearance of the so-called photonic band gap (PBG). Furthermore, when an artificial defect interrupts the periodicity of the PC, photon confinement can take place in the defect layer [3–6]. By inserting a third dielectric material as a defect layer in the PC structure, narrow spectral windows, corresponding to the defect modes, can be generated in the PBG. Utilizing the properties of defect modes [5], various applications such as narrow-bandpass filters [4], low-threshold lasers [7] and fluorescence enhancement devices [8] have been demonstrated. Conventionally, the way to produce defect modes is through prefabrication of a defect layer in a PBG material; for example, infiltration with anisotropic liquid crystal (LC) in a multilayer PC [9]. Such defect modes, though tunable, are often persistent due to the permanent existence of the defect layer.

Recently, chiral mesogens like cholesteric LCs (CLCs) [10,11] have received much attention as self-organized PCs. CLCs possess molecular chirality and form helical structures spontaneously. Their unique properties include optical stability, tunability and switchability. CLC molecules align themselves homogeneously in the plane perpendicular to the helical axis and rotate the director continuously along the helical axis. In such a helical structure, circularly polarized light with the same handedness as the helix propagating along the helical axis is selectively reflected and a stop band results [12]. Additionally, dual-frequency CLCs (DFCLCs), often made of mixtures of dual-frequency nematic LCs and chiral dopants (CDs), are characterized by their frequency-revertible dielectric anisotropy $\Delta\varepsilon$ that changes from positive to negative with rising frequency beyond a certain value; i.e., the crossover frequency f_c. Based on this characteristic, DFCLCs have been suggested for photonic applications [13–19] including light shutters [16,17] and displays [18,19]. Lately, a drive scheme involving the thermodielectric effect in a DFCLC system has been reported [20]. In a high-frequency electric field, the dielectric heating leads to the increases in temperature T as well as in f_c, reversing the sign of $\Delta\varepsilon$ at the very frequency and subsequently changing the optical state of the DFCLC. In this work, we exploit the thermodielectric effect to locally deform the helix in the middle portion of the CLC and, hence, manipulate the defect modes. We show, for the first time to the best of our knowledge, that thermodielectro-induced defect modes (TIDMs) can be realized for switchability and tunability in DFCLCs.

The helical pitch of a CLC depends on T, so a local deformation of helix can be effectively induced by dielectric heating. The cell boundaries near the surrounding air are at a relatively lower temperature. Thus, a certain spatial variation in pitch is anticipated. The strong surface anchoring keeps the pitch barely changeable near the boundary sides when the dielectric heating affects the CLC structure. These two reasons lead to the local deformation, yielding an induced defect layer in the middle. This locally thermo-prompted molecular deformation in pitch caused by a frequency-modulated voltage is conceptually shown in Fig. 1. The substantial temperature gradient caused by dielectric heating is the key to induce the significantly local pitch deformation and, in turn, the defect-mode spectrum.

#203354 - $15.00 USD Received 18 Dec 2013; revised 3 Feb 2014; accepted 3 Feb 2014; published 6 Feb 2014

2. Experimental

The DFCLC used was a mixture of the CD S-811 (Merck) with left handedness and the nematic MLC-2048 (Merck) with the clearing point 110 °C and $\Delta\varepsilon = 2.8$ at 1 kHz and 25 °C. The CD concentration was 20 wt%. The mixture was injected into empty planar-alignment cells by capillary action in the isotropic phase. Each cell comprised a pair of 1.1-mm-thick indium–tin-oxide glass substrates coated with alignment layers, yielding a cell gap d of 11 ± 0.5 μm. The frequency f of the applied voltage was fixed at 100 kHz. The transmission spectra of the LC cells were acquired with a spectrophotometer (Ocean Optics HR2000 +). All experimental data were measured at an ambient temperature of 26 ± 1 °C and the unperturbed pitch was 395 nm. When an electric field **E** is applied across a LC cell, it imposes a torque on the director $\hat{n}$, depending on $\Delta\varepsilon = \varepsilon_{\parallel} - \varepsilon_{\perp}$, where $\varepsilon_{\parallel}$ and $\varepsilon_{\perp}$ denote the relative permittivity components in the cases of $\hat{n} \parallel \mathbf{E}$ and $\hat{n} \perp \mathbf{E}$, respectively. Note that $\Delta\varepsilon$ is an explicit function of f for a DFCLC material. When a low-f ($< f_c$) field is applied, $\Delta\varepsilon > 0$ and $\hat{n}$ tends to be parallel to the field direction. In contrast, $\Delta\varepsilon$ becomes negative and $\hat{n}$ tends to be perpendicular to the field when the DFCLC is in a high-f ($> f_c$) **E**. The strength of the thermodielectric effect is determined by the efficiency of absorption of electromagnetic wave by the dielectric bulk. Here the dielectric heating is manifested through reorientation of the LC molecular dipoles, which is especially significant at high frequencies ($f > f_c$) [21].

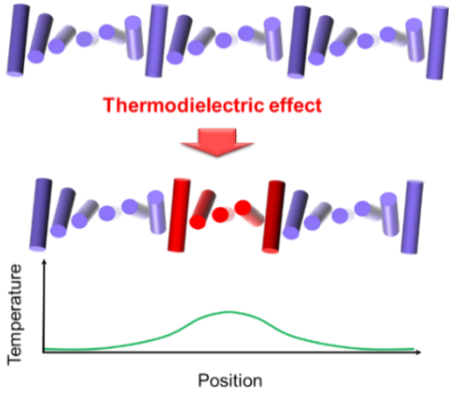

Fig. 1. Conceptual schematic of a local-deformation-induced photonic defect layer in a DFCLC by the thermodielectric effect.

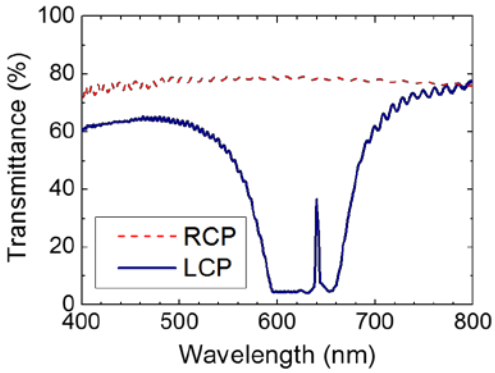

Fig. 2. Transmittance spectra of a DFCLC containing a deformation-induced defect layer for RCP (red dotted line) and LCP (blue solid curve) light. The unperturbed pitch is about 400 nm.

#203354 - $15.00 USD Received 18 Dec 2013; revised 3 Feb 2014; accepted 3 Feb 2014; published 6 Feb 2014

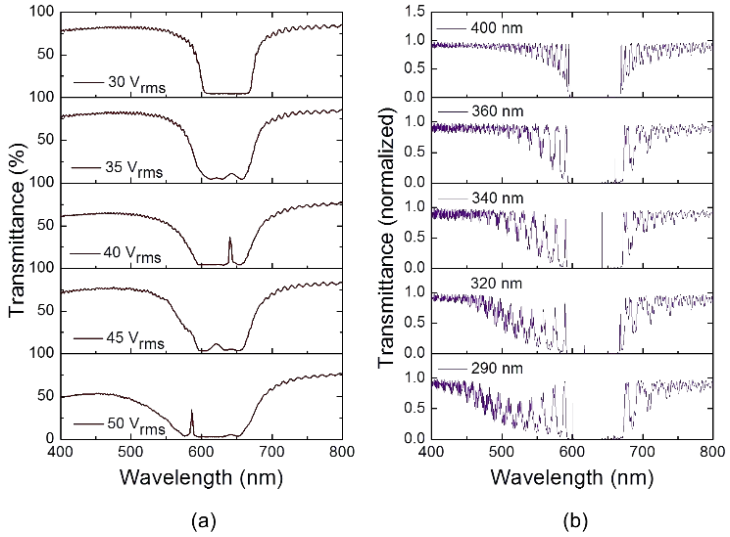

Fig. 3. Transmission spectra of LCP light going through a DFCLC possessing defects induced by dielectric heating (a) at various applied voltages (experimental data) and (b) compared to various pitch values in the middle defect layer (simulated data).

3. Results and discussion

Figure 2 shows two typical transmission spectra when left circularly polarized (LCP) light and right circularly polarized (RCP) light passed through a DFCLC containing a thermodielectro-induced defect layer (TIDL). It is clear that the LCP light was reflected within the PBG owing to the chirality of S-811 and, in turn, of the DFCLC to be left-handed. Note that the deformation-induced change in pitch gave rise to a TIDM window of ~3.9 nm in full width at half maximum (FWHM) in the PBG for the LCP light. According to our simulation, the FWHM of such window decreases with increasing thickness or decreasing pitch of the central TIDL. The experimental spectra of the DFCLC in various heating conditions are also shown in Fig. 3(a). A transmission peak originating from the TIDL was observed in the stop band for the LCP case. Due to the thermodielectric effect, a pronounced TIDM first appeared at the wavelength of 640 nm as the voltage increased to 40 V_{rms}. The spectral peak then blueshifted to *ca*. 585 nm at 50 V_{rms} because of the higher oscillation heating power resulting in a shorter pitch in the middle layer. There is no doubt that the heating time was an important variable in the experiment. For simplicity, we measured each spectrum after a voltage was continuously applied for 30 s. To further inspect the interplay between the TIDM and the local deformation of the pitch, simulations were performed and the results are depicted in Fig. 3(b). Here the spectral profiles were calculated by using the commercial software DIMOS, which is based on the extended 2 × 2 Jones matrix and 4 × 4 Berreman matrix. By decreasing the pitch from 400 to 290 nm (as labeled in the legend) for a distance of 1.375 μm in the middle, one can see that the simulated data roughly resemble the experimental spectra. A high voltage enhanced the thermodielectric effect. The pitch was, accordingly, shortened and optical path length reduced in the middle (defect) layer at a resulting high temperature, giving a blueshifted TIDM.

Figure 4 illustrates how the wavelength of the TIDM varied with the energy density and the defect-layer pitch. The dielectric heating energy density H_e of the bulk is calculated by

$$H_e = P \cdot t = \omega \varepsilon_0 \varepsilon''(\omega) E^2 \cdot t = \frac{2\pi f t \varepsilon_0 \varepsilon''(\omega) V_{rms}^2}{d^2}, \quad (1)$$

where P is the heating power density, t is the heating time, ω is the angular frequency of the applied voltage, ε_0 is the permittivity in vacuum, ε'' is the imaginary part of the complex

#203354 - $15.00 USD Received 18 Dec 2013; revised 3 Feb 2014; accepted 3 Feb 2014; published 6 Feb 2014

dielectric constant, and V_{rms} is the root-mean-square voltage. Equation (1) corresponds to an ideal condition; it can be, nevertheless, used to describe the observed behavior.

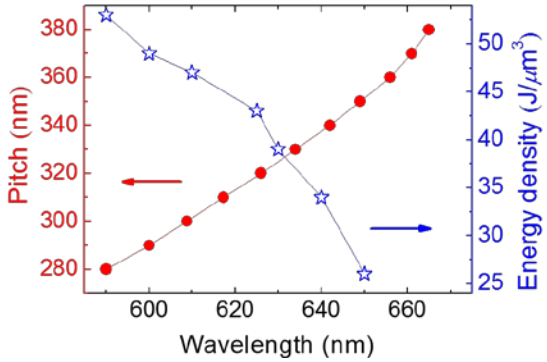

Fig. 4. Wavelength of the TIDM varying with the energy density and simulated pitch of the middle defect layer. The symbols show the experimental (blue) and the simulated (red) results.

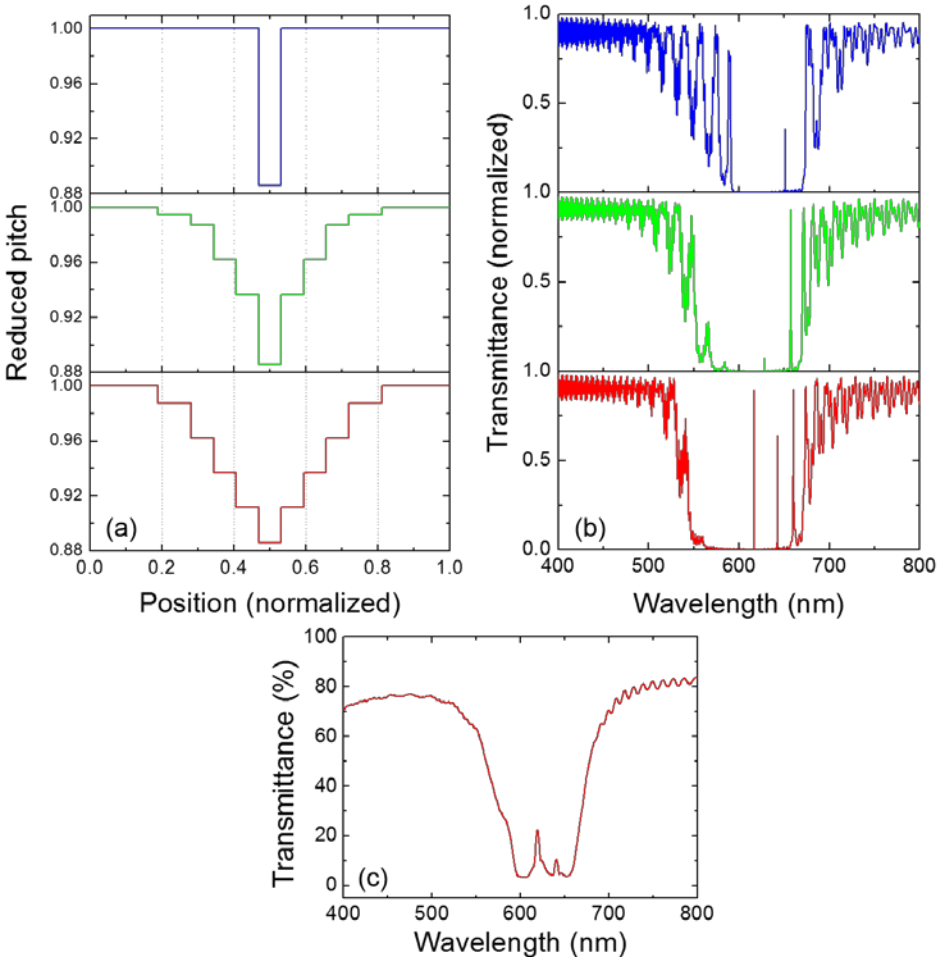

Fig. 5. (a) Three considered spatial variations of the pitch in a DFCLC. (b) Simulated spectra under the distinct conditions of the pitch as given in (a). (c) Experimental spectrum obtained in a specific pitch-deformation process exhibiting two defect-mode peaks in the PBG.

#203354 - $15.00 USD Received 18 Dec 2013; revised 3 Feb 2014; accepted 3 Feb 2014; published 6 Feb 2014

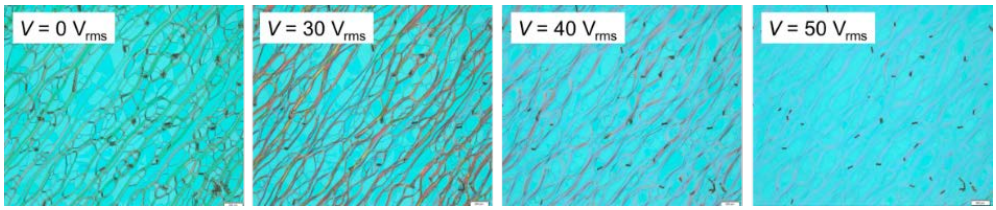

Fig. 6. Optical textures of a DFCLC at various applied voltages.

To approximate a more realistic case for the dielectric-heating-induced pitch variation in the simulation, different spatial distributions of the pitch were considered. The CLC was divided into 10 layers with the pitch configurations as shown in Fig. 5(a). One can see that a second defect mode appears and the PBG expands as the gradient of the pitch becomes smaller (Fig. 5(b)). Since a smoother distribution may be considered as a structure with a thicker defect layer, this can be understood as a result of the increment in effective optical defect thickness. Figure 5(c) depicts an experimental spectrum of a DFCLC under a prolonged heating time (50 V_{rms} for 50 s) for a smaller temperature gradient in the cell. This result is qualitatively in good agreement with the prediction by the simulation. It is important to mention that the defect-mode spectral profile is determined by a number of factors. The thermo-hydrodynamics fundamentally governs the properties of TIDMs. If the power of dielectric heating is higher, causing the thermal transition to be faster, then a non-ideal plural-peak spectrum can be encountered more frequently. On the contrary, under relatively lower applied voltage, the ideal single-peak mode lasts much longer in general.

Figure 6 presents crossed-polarizing micrographs of a 20-wt% DFCLC sample imposed by various voltages at 100 kHz. The initial planar state at 0 V_{rms} was characterized by many thick oily streaks. Colorful oily streaks then appeared at 30 V_{rms} in that the LC molecules started to rotate in the oily defects. Finally the texture exhibited seemingly fewer defects when the voltage was over 50 V_{rms} because of the negative dielectric torque. It is obvious from the optical textures that the images became brighter at 40–50 V_{rms}, implying the change in pitch; that is, the middle-layer deformation, of the DFCLC. Our observation indicated that, as long as the optical texture was identical, the spectral profile of the defect mode(s) was indifferent although the oily streaks would regain their darker colors very slowly in a voltage transition from a prolonged high voltage to a low voltage. The reason why the quenching did not work was presumably due to the complexity of the oily network structure caused by the high CD concentration used in this study. It is also worth mentioning that TIDMs are difficult to demonstrate or become stabilized. Since the thermodielectro-induced temperature gradient changed over time in a dynamic process before a state of thermal equilibrium was reached, the TIDMs were only observed for a few minutes. However, this problem can be solved with the technique of polymer stabilization for enhanced stability of TIDMs [22].

4. Conclusions

Based on the thermodielectric effect, we have demonstrated that photonic defect modes can be generated and that the switching and tuning of them can be realized by local deformation of the helix in the middle layer of a DFCLC. An external voltage at a high frequency applied across the thickness of the DFCLC cell can supply sufficient heat to induce a defect layer owing to the changed pitch susceptible to the local temperature in the middle. The defect modes appeared only when the incident circularly polarized light had the same handedness as the CLC. The tuning of the defect mode can be performed by local compression of the defect-layer helix, allowing the defect mode to blueshift. By controlling the extent of the modulation of the helix, a continuous shift of the defect mode can be achieved using the self-organizability of DFCLC without prefabrication of an artificial defect layer. On the basis of our approach, various potential applications can be expected such as reversible tuning of the

#203354 - $15.00 USD Received 18 Dec 2013; revised 3 Feb 2014; accepted 3 Feb 2014; published 6 Feb 2014

defect modes, single-mode lasing, monochromatic selection, lab-on-a-chip devices and optical communications.

Acknowledgments

This research is financially supported by the National Science Council of Taiwan under Grant Nos. NSC 101-2112-M-009-018-MY3 and NSC 103-2923-M-009-003-MY3.

#203354 - $15.00 USD Received 18 Dec 2013; revised 3 Feb 2014; accepted 3 Feb 2014; published 6 Feb 2014